Davidsmithite, $(Ca,\square)_2Na_6Al_8Si_8O_{32}$: a new, Ca-bearing nepheline-group mineral from the Western Gneiss Region, Norway

Sid-Ali Kechid[1], Gian Carlo Parodi[2], Sylvain Pont[2] and Roberta Oberti[3,*]

[1] Département de Géologie, FSTGAT-USTHB, BP, 32 El Alia, Bab Ezzouar, Alger, Algeria
[2] Laboratoire de Minéralogie, Département d'Histoire de la Terre, Muséum National d'Histoire Naturelle (MNHN), CP 52, 61 Rue Buffon, 75005 Paris, France
[3] CNR-Istituto di Geoscienze e Georisorse, Sede Secondaria di Pavia, via Ferrata 1, 27100 Pavia, Italy
*Corresponding author, e-mail: oberti@crystal.unipv.it

Abstract: Davidsmithite, a newly approved feldspathoid mineral (IMA 2016-070), occurs as a rock-forming mineral in the Liset eclogite pod (Norwegian Caledonides). It is transparent, colourless, uniaxial negative, $\omega = 1.538(2)$, $\varepsilon = 1.535(2)$. No cleavage was observed. Davidsmithite is hexagonal, space group $P6_3$ and has unit-cell dimensions: $a = 9.982(1)$ Å; $c = 8.364(2)$ Å; $V = 721.74$ Å^3; $Z = 1$; the $c{:}a$ ratio is 0.8379; the calculated density is 2.597 g cm^{-3}. The approved electron-microprobe analysis gave the crystal–chemical formula: $([Ca_{0.636}\square_{0.636}]\square_{0.414}K_{0.165}Na_{0.149})_{\Sigma2.000}Na_{6.000}(Al_{7.863}Fe^{3+}_{0.019})_{\Sigma7.882}Si_{8.192}O_{32}$ (where $\square$ = vacancy). Davidsmithite completes the compositional space of the nepheline-structure group by providing a new root-composition, $(Ca\square)_2Na_6Al_8Si_8O_{32}$. It is the Ca-analogue of classical nepheline, to which it is related by the heterovalent substitution of K^+_2 by $[Ca^{2+}\square]$. Most of the Ca^{2+} ions are situated in the same atomic position as K^+ in nepheline, but some occur in a new and disordered (Ca) atomic position, whose centre is shifted by 2.18 Å along the 6-fold axis. The studied samples show some solid-solution towards the other two possible end-members of the nepheline compositional space, so that the channel site contains all of Ca and K in the unit formula, with some Na and $\square$. In the Liset eclogite pod, davidsmithite occurs in retrogressed, formerly jadeite-rich zones; it commonly overgrows lisetite and is associated with albitic plagioclase and taramitic amphibole. This eclogite occurrence is noted for its bulk-rock compositions rich in (Na + Al) and poor in (K + Mg). The paucity in K prevented the growth of nepheline, and the paucity in Si in precursor jadeite led to the growth of a feldspathoid (davidsmithite) as well as of lisetite; a feldspar (albite or oligoclase) also occurs nearby.

Key-words: davidsmithite; new mineral; crystal structure; EMP analysis; Raman spectroscopy; Ca-silicate; nepheline group; feldspathoid; Liset eclogite pod; Norway.

1. Introduction

The new mineral davidsmithite, with ideal chemical composition $(Ca\square)_2Na_6Al_8Si_8O_{32}$ (where $\square$ = vacancy), has recently been recognised by the International Mineralogical Association (IMA; vote 2016-070). It has the nepheline framework, but Ca^{2+} and vacancy (in equal proportions) are found to substitute for K^+_2 in the channels; because of this heterovalent substitution, davidsmithite is a new end-member of the nepheline group (see Deer *et al.*, 1992 for a group description). This paper presents all the data submitted to the IMA for the approval, along with a few extra comments useful to describe the chemical and crystallographic relationships of davidsmithite to relevant mineral phases and more information on its occurrence in the retrogressed Na–Al-rich K–Mg-poor Liset eclogite pod in the Norwegian Caledonides (Smith, 1988). This is the same type locality as that of lisetite, ideally $CaNa_2Al_4Si_4O_{16}$, a tectosilicate with a structure somewhat related to feldspars (Rossi *et al.*, 1986; Smith *et al.*, 1986); indeed these two minerals are

commonly associated, davidsmithite overgrowing lisetite in corona textures. The name davidsmithite honours the important contributions to mineralogy and petrology provided by David Christopher Smith (born 1946), Emeritus Professor at the Muséum National d'Histoire Naturelle (MNHN) in Paris, France. As a mineralogist, he (together with the CNR team in Pavia led by the late Giuseppe Rossi and Luciano Ungaretti) discovered the new minerals nyböite, lisetite, taramite and ferro-taramite in Norway (Ungaretti *et al.*, 1981; Rossi *et al.*, 1986; Smith *et al.*, 1986; Oberti *et al.*, 2007). As a petrologist, he pioneered the recognition of the new sub-discipline of UHPM (Ultra High Pressure Metamorphism) (Smith, 1976; Lappin & Smith, 1978), well before coesite was found in Italy (Chopin, 1984) and in Norway (Smith, 1984). He also created the COSEM collection (Collection David Smith des Eclogites du Monde) at the MNHN.

After the recent recognition of trinepheline, a feldspathoid mineral with Na^+_2 substituted for K^+_2 in nepheline thus giving Na = 8 atoms per formula unit (apfu) for O = 32 apfu (Ferraris *et al.*, 2014; *cf.* Johan *et al.*, 2017,

Table S4), the mineral described in Rossi *et al.* (1989) as a "K-poor Ca-rich silicate with the nepheline framework" has become representative of the $(Ca^{2+}\square)$ corner in the K–Na–Ca sub-triangle of the feldspathoid compositional space occupied by the nepheline group. This is represented in Fig. 1 on the basis of 32 O apfu, where the corner $K_2 Na_6$ is classical nepheline, the corner $Na_2 Na_6$ is trinepheline, and the corner $(Ca\square) Na_6$ is davidsmithite. In other words, the two-dimensional K–Na join of nepheline compositional space linking nepheline to trinepheline is now opened up into the K–Na–$(Ca\square)$ sub-triangle. The presence of the heterovalent substitution $K^+_2 \rightarrow Ca^{2+} + \square$ implied the need for a new root name at the $(Ca\square)$ corner. We introduce here the three-letter symbol "Dvs" for davidsmithite, and "Trn" for trinepheline. We use the symbol "Lis" for lisetite instead of "Lt" (Smith *et al.*, 1986) to follow the modern choice of using three-letter symbols, with Nph for nepheline and Kls for kalsilite taken from Whitney & Evans (2010).

Figure 1 is not a simple, purely chemical, normalised at% Ca–Na–K plot, such as the standard An–Ab–Or feldspar plot of Ca–Na–K in at%; it is a charge-balanced chemical $(Ca\square)$–Na_2–K_2 plot in at%, projected from the $\square_8Si_{16}O_{32}$ apex of tridymite (*cf.* Fig. 1b in Rossi *et al.*, 1989) such that here $Al_8Si_8O_{32}$ is constant everywhere, and where, in order to present the nepheline-structure system in an equilateral sub-triangle at the top, the atomic concentration of Ca must be coupled with an equal amount of vacancy. In this diagram, anorthite $(CaAl_2Si_2O_8)$, expressed on the same $Al_8Si_8O_{32}$ basis as nepheline, lies at the $Ca_4\square_4$ apex. This equilateral sub-triangle facilitates the expression of the crystal–chemical relationships, thus improving the visibility of the nepheline-group species. Davidsmithite $(Ca\square)Na_6Al_8Si_8O_{32}$ is chemically equivalent to 75 mol% $Na_8Al_8Si_8O_{32}$ (trinepheline) + 25 mol% $Ca_4Al_8Si_8O_{32}$ (anorthite). In contrast, lisetite has 50% of each. Note that lisetite would occupy the 33.33:66.66% position in a purely chemical plot.

The 50:50 rule for nomenclature boundaries presently used for mineral groups is applied here for the nepheline-structure system (Fig. 1), and each of the three species has a different dominant cation (K or Na or $(Ca_{0.5}\square_{0.5})$) in the channel. These boundary limits for the mineral species were also approved by the above-mentioned IMA 2016-070 vote.

2. Occurrence and petrology

Davidsmithite was discovered at the Liset eclogite pod, Liset, Selje, Western Gneiss Region (WGR), Vestlandet, Norway (Lat. 62°4′ N, Long. 5°20′ E). The eclogite pod at Liset lies within the Norwegian Coesite-Eclogite Province (Smith, 1984, 1988), which since then has focused considerable attention and was refined and extended (*e.g.*, Wain, 1997; Hacker, 2007). In the holotype rock sample G201, the new mineral occurs closely associated with Lis, the other compositionally similar but structurally different tectosilicate lisetite $(CaNa_2Al_4Si_4O_{16})$ discov-

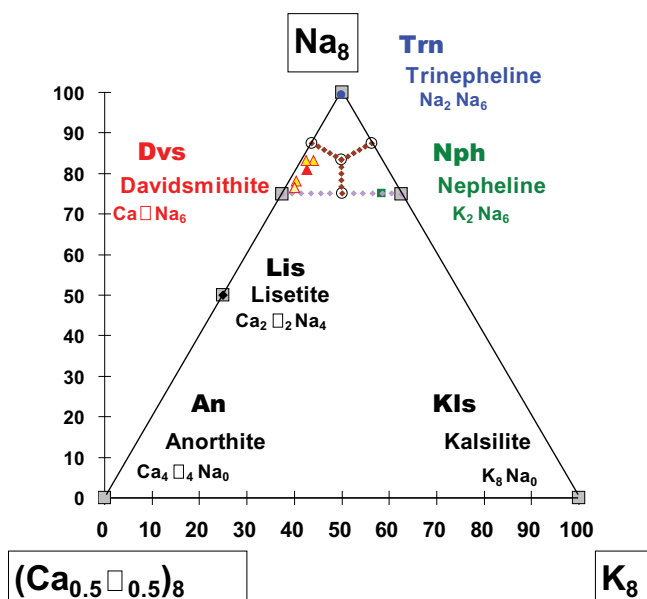Fig. 1. The charge-balanced $Ca_{0.5}\square_{0.5}$–Na–K chemical plot (in at%), where $Al_8Si_8O_{32}$ is constant in all the large triangle (modified after Rossi *et al.*, 1989). The dotted purple line delineates the limit of the "small triangle" of the nepheline-structure group. Large grey squares = end-member compositions relevant to the present discussion. Solid lozenge = lisetite (type specimen from Rossi *et al.*, 1986); red triangle = davidsmithite (this work); yellow triangles = four other analyses of davidsmithite from the same locality; blue circle = trinepheline (type specimen from Ferraris *et al.*, 2014); green square = nepheline (representative sample no. 2 on page 478 in Deer *et al.*, 1992). Open circles and small brown dotted lozenge lines: 50:50 boundaries in the compositional space of the nepheline structure, as first suggested by Rossi *et al.* (1989) and now approved by the IMA along with the new mineral Dvs. In this diagram, fabriesite would plot over trinepheline, but it is a hydrous mineral with a different crystal structure. See text for more details.

ered in retrogressed jadeite-rich layers in the same Liset eclogite pod (Kechid, 1984; Kechid & Smith, 1985; Rossi *et al.*, 1986; Smith *et al.*, 1986). Smith (1988) reviewed the "peculiar mineralogy" of eclogites in the Norwegian Coesite-Eclogite Province and WGR and provided a comprehensive bibliography. Kechid (1984) and Kechid & Smith (1985) summarised the petrological evolution of the Liset eclogite pod.

The closest directly associated phases are the tectosilicates lisetite and albitic plagioclase (Fig. 2), along with the monoclinic amphibole taramite. Sometimes Dvs can be seen to be replacing a cluster of Lis at its edges (see Fig. 1 in Smith *et al.*, 1986) in an irregular corona style, but the more regular texture of Fig. 2, where Dvs seems to be pseudomorphing Lis, is rare. Relict jadeite and quartz, armoured by coronas of clinoamphibole, occur nearby.

The complete list of associated minerals in the Liset Eclogite pod is long because this retrogressed, extremely Na- and Al-rich eclogite contains many symplectites after the principal eclogite-facies phases. World-wide many of these phases are still rare (Al–F-rich titanite – Smith & Lappin, 1982; nyböite – Oberti *et al.*, 1989, 2003; preiswerkite – Oberti *et al.*, 1993; taramite – Oberti *et al.*,
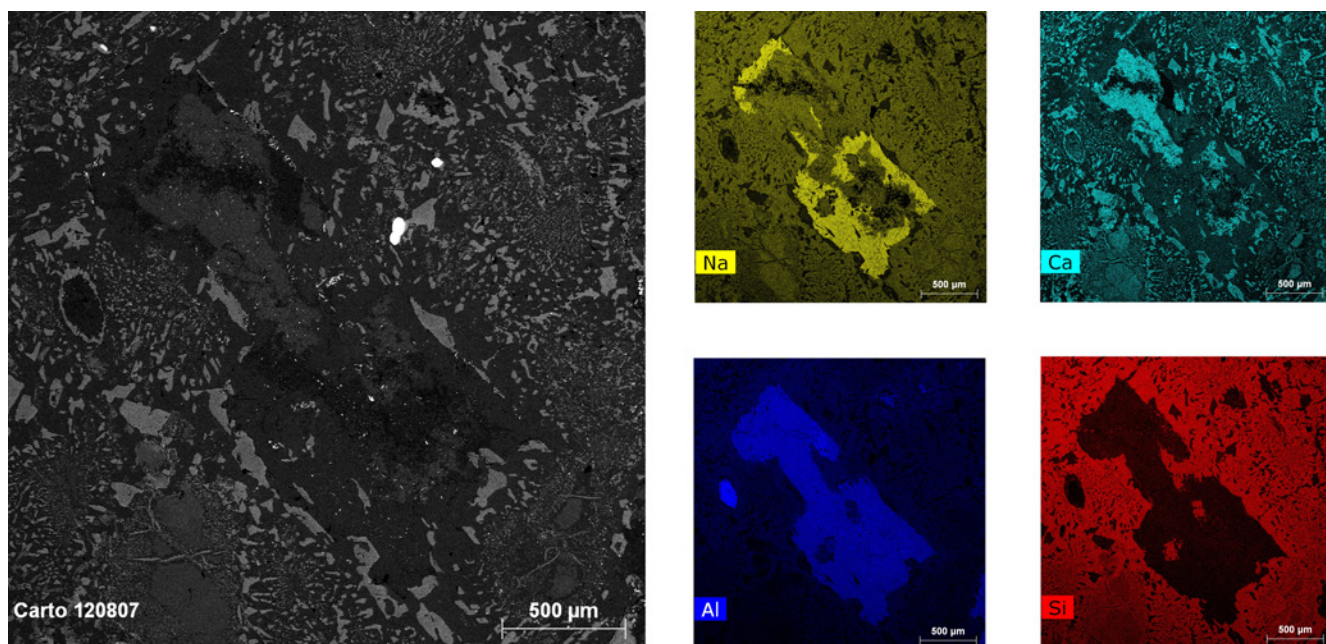
Fig. 2. A SEM back-scattered electron image showing, in the centre, an oblique lath of intimately associated davidsmithite (Dvs, darker, outermost) and lisetite (Lis, lighter, innermost). This feature is clearly shown by the elemental maps in colour: Dvs is richer in Na than Lis, whereas the Al and Si contents are similar in the two minerals. The matrix outside this lath is dominated by symplectitic albitic plagioclase (darker) with amphiboles and micas (lighter).

2007; ferro-taramite – Ungaretti *et al.*, 1985) or still even unique (lisetite – Smith *et al.*, 1986). The complete list (after Kechid, 1984; Smith, 1988) includes garnet, jadeite, omphacite, aegirine, kyanite, coesite (relict textures thereof), quartz, albitic plagioclase, lisetite, taramite, ferro-taramite, nyböite, preiswerkite, eastonite, muscovite, paragonite, margarite, chlorite, zoisite, clinozoisite, epidote, allanite, staurolite, magnetite, rutile, ilmenite, hematite, corundum, Al–F-rich titanite, apatite, zircon, late zeolitic products. Liset is the holotype locality for taramite, ferro-taramite, lisetite and now davidsmithite. Smith (1988) described the Norwegian Coesite-Eclogite Province as "a mineralogist's paradise and a petrologist's nightmare"; the Liset eclogite pod is probably the best example thereof.

Davidsmithite and lisetite both occur in the retrogressed part of the Liset eclogite pod where the key eclogite-facies minerals garnet + clinopyroxene + kyanite were amphibolitised during decompression. Instead of the usual symplectites of albitic plagioclase and pargasitic amphibole, typical of most eclogites world-wide, the very Al-rich (kyanite + jadeite)-rich zones at Liset are replaced by taramite + lisetite + davidsmithite, taramite + albitic plagioclase, preiswerkite + albitic plagioclase, corundum + albitic plagioclase, all except corundum being rich in both Na and Al (Kechid, 1984; Smith, 1988). Davidsmithite was also found to occur without lisetite in other layers of the Liset eclogite pod.

No other record is known of a nepheline-group member composition with dominant (Ca□) end-member than the X-ray diffraction study of Rossi *et al.* (1989), in which no name was proposed. Therefore, world-wide, davidsmithite is still a mineral species unique to its Liset occurrence, as is apparently also the case for lisetite.

3. Type material

The eclogite sample labelled G201 deposited in the rock collection COSEM of the MNHN is the source for the thin section (original number G201b7) in which both Lis and Dvs were found. This thin section, now officially labelled MNHN215-001, represents the type material source for both phases and is deposited in the Mineral Collection of MNHN. The thin section 7, made from horizon 7 of the rock fragment *b* of the original rock specimen G201, was used for the electron-microprobe (EMP) analyses of Dvs and Lis. The crystal used for the X-ray structure refinement (Rossi *et al.*, 1989) was picked up from a small piece of rock from the same horizon G201b7. The new scanning electron microscope (SEM) maps provided in this work have been obtained on the same thin section.

4. Experimental results

4.1. EMP analysis

Table 1 gives the mean values and ranges of ten spot analyses of Dvs obtained from the type sample G201b7 and recorded with a Cameca CAMEBAX electron microprobe (1 μm sized electron beam, 15 kV, 12 nA) at the MNHN. No other elements were detected in a wavelength scan over all elements with $Z > 10$. No wet-chemical tests were done because of the small size of crystal grains. Significant F and Cl content were not found in any of the crystals used for crystal structure refinement, which is consistent with the lack of sites suitable for OH, F and Cl in the nepheline structure. However, in some other crystals of Dvs analysed later by EMP, a maximum
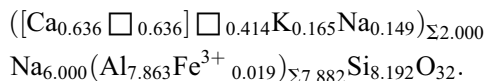
Table 1. Electron-microprobe analysis (mean of 10; wt%) for davidsmithite.

Oxide	Mean	Range	Standard
CaO	3.16	3.10–3.22	Wollastonite
K_2O	0.69	0.56–0.81	Orthoclase
Na_2O	16.89	16.85–16.92	Albite
Al_2O_3	35.52	35.42–35.61	Corundum
Fe_2O_3	0.13	0.07–0.19	Hematite
SiO_2	43.63	43.06–44.21	Wollastonite
MgO	0.02	0.00–0.05	Forsterite
MnO	0.04	0.00–0.07	Rhodonite
NiO	0.01	0.00–0.01	Ni-oxide
TiO_2	0.04	0.00–0.08	Rutile
Total	100.12		

amount of 0.10 wt% F ($= 0.06$ F apfu) was recorded. Several crystals were analysed to examine chemical variations (Fig. 1).

Raman analysis provided no indications of OH. Notably, the presence of water is incompatible with the nepheline structure, and would imply a very different structural arrangement with large cavities as in fabrièsite (Ferraris *et al.*, 2014), ideally $Na_3Al_3Si_3O_{12} \cdot 2H_2O$, a hydrate mineral with, otherwise, the same chemistry as trinepheline but with a completely different structure.
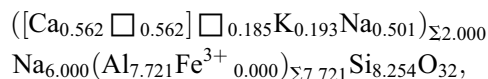
The empirical formula obtained from the average analysis of Dvs in Table 1, calculated on the basis of 32 O apfu, is:

$$([Ca_{0.636} \square_{0.636}] \square_{0.414} K_{0.165} Na_{0.149})_{\Sigma 2.000}$$
$$Na_{6.000}(Al_{7.863}Fe^{3+}_{0.019})_{\Sigma 7.882}Si_{8.192}O_{32}.$$

Iron is in the trivalent state according to the usual practice for feldspars and feldspathoids (Deer *et al.*, 1992). MgO, MnO, NiO, Cr_2O_3 and TiO_2 have concentrations less than 0.10 wt% each (Table 1) and were ignored: (a) because they are attributed to contamination from Mg–Ti-rich micro-inclusions that do occur in Dvs, and (b) because their respective cations have no suitable atomic site in Dvs (as in the other tectosilicates Lis and in the feldspars). The value of 0.10 wt% of any of the contaminant elements, that leads to around 0.01 apfu, was chosen as a cut-off level for rejecting a whole analysis. Most analyses of Dvs (and also of Lis) reveal traces from 0.100 wt% down to 0.001 wt% and it was considered desirable to keep these analyses with insignificant impurities in order to have a larger dataset for examining the more important variations in K–Na–Ca contents. Vacancies due to the heterovalent substitution of K^+_2 by $[Ca^{2+}\square]$ are kept separated from the other vacancies which are related both to minor Si excess over Al (as noted also by Deer *et al.*, 1992 for many feldspathoids) and to a slight deficiency of total alkalis with respect to $(Al + Si)$. The key point is that in the "hexagonal" channel, Ca^{2+} is dominant over K^+ and Na^+, and is also associated with vacancy. The simplified ideal
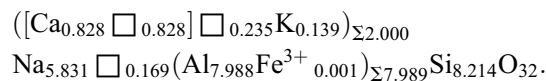
formula of davidsmithite is: $(Ca\square)_2Na_6Al_8Si_8O_{32}$, which requires (in wt%) CaO 4.96, Na_2O 16.45, Al_2O_3 36.07, SiO_4 42.52, summing to 100 wt%.

Rossi *et al.* (1989) published another mean-of-ten EMP analysis (the uppermost cross in Fig. 1) which provides a slightly different formula,

$$([Ca_{0.562} \square_{0.562}] \square_{0.185} K_{0.193} Na_{0.501})_{\Sigma 2.000}$$
$$Na_{6.000}(Al_{7.721}Fe^{3+}_{0.000})_{\Sigma 7.721}Si_{8.254}O_{32},$$

which however falls within the Dvs compositional space. Further EMPA analyses revealed that some solid solution is present mainly along the $(Ca_4\square_4)$–Na_8 join, at nearly constant K content (see the other crosses in Fig. 1).

An analysis acquired after the submission to the IMA for the species recognition is even richer in Dvs (the lowermost cross in Fig. 1) since its shows more Ca and Al, and less K, Na, Fe^{3+} and vacancies than the "type" analysis as recognised by the IMA, with no Na in the extra-framework site and a little shortage in the six-fold site. Its formula is:

$$([Ca_{0.828} \square_{0.828}] \square_{0.235} K_{0.139})_{\Sigma 2.000}$$
$$Na_{5.831} \square_{0.169}(Al_{7.988}Fe^{3+}_{0.001})_{\Sigma 7.989}Si_{8.214}O_{32}.$$

4.2. Physical and optical properties

Davidsmithite generally occurs as anhedral, and rarely skeletal or lath-like, crystals up to 80–100 μm long and about 30 μm wide in polycrystalline aggregates (Fig. 2). In hand specimen, Dvs is indistinguishable within a matrix of fine-grained minerals including colourless to light-grey lisetite, plagioclase and quartz. In thin section it has a lower birefringence than lisetite and albitic plagioclase and thus tends to be dark grey in a 30-μm-thick section under crossed polarisers. Twinning was not observed in thin section.

The submicrometre-sized inclusions in Dvs (as well as in Lis) can be defined as Mg–Ti-oxides from preliminary SEM work (Parodi & Pont, *in prep.*). The presence of Dvs within a sample can best be decrypted using SEM imaging systems. Secondary-electron images (not shown) clearly pointed out that Dvs, together with later zeolitic products, is softer and more sensitive to polishing-induced damages compared to amphibole.

Table 2 presents the physical and optical properties of Dvs that could be obtained. The small size of the crystals, the frequent intergrown textures with Lis, and/or the presence of micro-inclusions prevented the measurement of all of the desired properties.

Davidsmithite is colourless to pale yellowish in thin section, and has a low birefringence; it is thus similar to Lis and albitic plagioclase. The best optical indication of Dvs is its low birefringence. It can be easily recognised when intergrown with Lis, but when occurring in the rock matrix, the presence of Dvs can only be confirmed by EMP or SEM analysis.

Table 2. Physical, optical and crystallographical properties of davidsmithite.

Physical	*Optical*[c]
Colour: white, transparent	Colourless to yellowish
Streak: white	Uniaxial (−)
Lustre: vitreous, greasy	$\omega = 1.538(2)$
Non-fluorescent	$\varepsilon = 1.535(2)$
Hardness (Mohs): <5.5[a]	
Cleavage: none	*Crystallography*
Parting: not observed	System: hexagonal
Fracture: not observed	Space group: $P6_3$
Density (calc.) = 2.597 g cm^{-3}[b]	$a = 9.982(1)$ Å
	$c = 8.364(2)$ Å
Compatibility	$V = 721.74$ Å^3
$1 - (K_P/K_C) = -0.008$ (superior)	$Z = 1$
	$c{:}a$ ratio = 0.8379
Morphology	
Habit: irregular	
Forms: not observed	
Twinning: none observed in thin section[d]	

[a] Hardness (Mohs) deduced according to the behaviour during sample polishing.
[b] From single-crystal structure refinement (Rossi *et al.*, 1989).
[c] RI values were estimated from multiple Becke line tests with adjacent phases, and birefringence colours (white light).
[d] Twinning (probably polysynthetic) on $(1\,0\,0)$ is present in the crystal used for X-ray structure refinement; the two orientations occur in proportions of 95% and 5%, as deduced from the ratio I_{230}/I_{320} (Rossi *et al.*, 1989).

4.3. Raman spectroscopy

Raman spectra of Dvs in thin section G201b7 were recorded using a Renishaw model "Invia" Raman Spectrometer at the CRCC, MNHN, Paris, France (Fig. 3 and Table 3) with the following key operating conditions: Ar$^+$ 514.5 nm laser; 5–50 mW approx. laser power at the sample; 10 s counting time; five accumulations.

The spectrum of Dvs is quite different from those of the coexisting tectosilicates Lis (Boyer *et al.*, 1989) and albitic plagioclase. Both Trn and Fab (fabrièsite) also have different Raman spectra; in particular they both have strong Raman bands centred at about 450 and 490 cm^{-1} whereas Dvs has a strong wide "massif" centred distinctly lower, around 425 cm^{-1}, with a shoulder at 470 cm^{-1} that thus lies in "trough" between the mentioned bands at 450 and 490 cm^{-1} of the other two species. Also, Trn and Fab show several Si–O and/or Al–O bands at <970 cm^{-1} whereas Dvs has its T–O Raman bands at >970 cm^{-1}.

The spectra obtained from Dvs in the holotype thin section G201b7 clearly show superposed Raman spectra of the glass slide and of the epoxy resin (see "Spectral zones" in Table 3 and Fig. 3). Seven weak wide spurious "humps" between 1335 and 2390 cm^{-1} often occur as artefacts with the spectrometer used. Moreover, the wide signal around 1350 cm^{-1} and that just to the left of 1612 cm^{-1} might correspond to graphitic carbon in the carbon-coating.

No significant signal is observed from Dvs in the H–O–H and O–H stretching zone around 3500 cm^{-1}. The narrow band at 1612 cm^{-1} is characteristic of Araldite

epoxy resin; hence this is definitely not considered to represent a signal of O–H bending. Hence Dvs is anhydrous like Trn, as expected from inspection of its crystal structure and the fact that EMP analytical totals are in the range 99.0–100.5 wt%.

4.4. Crystallography

Table 2 also reports the basic crystallographic data available for davidsmithite. A detailed discussion of the results of the single-crystal structure refinement (SREF) of Dvs from the holotype section G201b7 had been reported in Rossi *et al.* (1989), to which the interested reader is referred.

Due to the paucity, small size, irregular morphology, presence of micro-inclusions and hence the general low quality of crystals, X-ray powder-diffraction data (Cu$K\alpha$, $\lambda = 1.54178$ Å) were obtained using the XPREP utility of SAINT (Bruker, 2003), which generates a 2D powder diffractogram (Debye–Scherrer technique) starting from the F_{obs} collected on the single-crystal and taking into account solely the information concerning the unit-cell dimensions and the Laue symmetry. No Lorentz and polarisation corrections were applied. Data are given in Table 4 together with a comparison with those measured for synthetic "Na-nepheline" and calculated for trinepheline (as taken from the ICDD database).

5. Discussion

5.1. Crystal-chemistry and relations with other species

As a complete discussion of the results of structure refinement was already published by Rossi *et al.* (1989), we provide here solely some comments, a sketch of the layers made of alternating "hexagonal" and "oval" six-membered rings of tetrahedra with *UDUDUD*-configuration (Fig. 4a) and a representation of the electron density in the channel defined by "hexagonal" rings of tetrahedra (Fig. 4b). The EMP and SREF analyses show that Dvs is a tectosilicate with the same Al–Si framework as $K_2Na_6Al_8Si_8O_{32}$ (Nph), but with different site populations and ordering for the K and Ca ions. Actually, the shape of the electron density inside this channel indicates an almost continuous positional disorder, with one maximum at 1.28 Å from the K site. This position (alternative with respect to that of K in Nph) allows a different and more suitable coordination for Ca and Na, with six oxygen atoms at an average ⟨Ca–O⟩ distance of 2.66 Å instead of the nine-coordinated K at an average corrected ⟨K–O⟩ distance of 3.02 Å (with the three longer distances equal to 3.044). Rossi *et al.* (1989) provided also distances corrected for riding motion (Busing & Levy, 1964) and recommended their use because of the extensive long-range disorder of the nepheline structure due to a list of factors, such as the presence of domains of Al/Si ordered rings of tetrahedra, of positional disorder of the channel cations and even of twinning. Their list of interatomic distances is reported in Table 5.
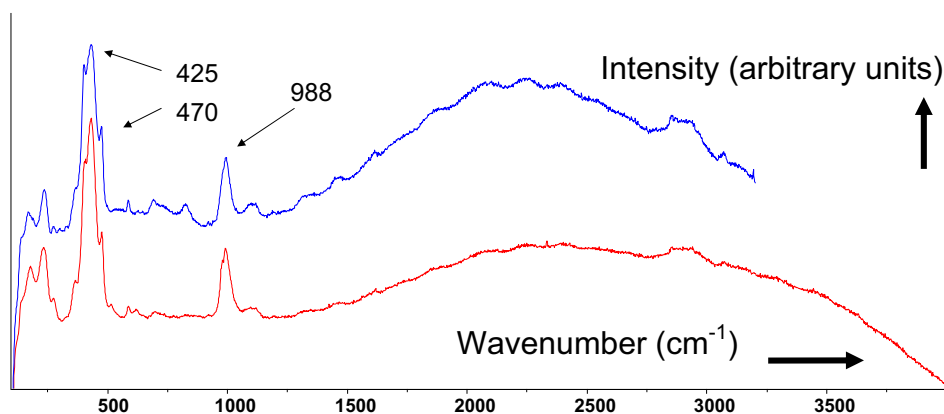
Fig. 3. Two Raman spectra of Dvs from slide G201b7 revealing strong bands at 228, 425 and 988 cm^{-1} (see Table 3 and the text for further comments).

Kahlenberg & Böhm (1998) showed that Trn (space group $P6_1$, $a = 9.995$, $c = 24.797$ Å) is a superstructure of Nph, with the tripling of the c lattice parameter due to modifications of the basic nepheline structure, namely a collapse in the symmetry of the "hexagonal" rings of Nph which results in relaxation of the framework and in an ordered distribution of the Na cations. Actually, the Na4 site of Trn is placed on the 6_1 axis, and is coordinated with eight O atoms at an averaged distance of 2.98 Å.

All the minerals discussed so far are anhydrous. Fabrièsite (Ferraris *et al.*, 2014), another mineral which may appear to be relevant to the chemical plot reported in Fig. 1 (unit formula $Na_3Al_3Si_3O_{12} \cdot 2H_2O$, orthorhombic, space group $Pna2_1$, $a = 16.426$ Å, $b = 15.014$ Å, $c = 5.223$ Å) was shown to be consistent with a topologically different structure, which had been refined on the synthetic analogue by Hansen & Fälth (1982). It consists in "a set of parallel two-repeat chains with alternating single and double chains built up by a regular alternation of AlO_4 and SiO_4 tetrahedra. This framework contains channels running along c, with elongated apertures consisting of eight-membered rings of tetrahedra". Therefore, although chemically related, Fab does not belong to the nepheline structural group.

Because the [8]-fold coordinated Na_6-occupied sites are common to all three species, the upper triangle in Fig. 1 is defined solely by the extra-framework large-cation-site atoms [K_2 or Na_2 *vs*. (Ca$\square$)], with the rest of the formula (namely $Na_6Al_8Si_8O_{32}$) being constant. Therefore, distinction between these three end-members is easy with good EMP analyses. However, it has been found that when Si is a little too high in EMP analysis, then the result will resemble the composition of a poor EMP analysis of plagioclase with Si a little too low. This is because the only purely chemical difference between the entire large triangle of Fig. 1 and the Ab–Or–An feldspar triangle is the SiO_2 concentration. Thus Trn + SiO_2 = Ab, and Kls + SiO_2 = Or, with the ratio (Na,K)/ Al = 1 everywhere:

$$(Na, K)_8Al_8Si_8O_{32} + 16SiO_2 = (Na, K)_8Al_8Si_{24}O_{64},$$
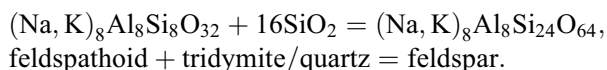feldspathoid + tridymite/quartz = feldspar.

Table 3. Wavenumbers (cm^{-1}) of two Raman spectra obtained from Dvs in the "type sample" thin section G201b7.

Spectrum no. DSP10-T10A5_01	Spectrum no. DSP100-T10A5-02	Spectral zones
⟨173⟩	⟨173⟩	
⟨227⟩	⟨227⟩	
(270)	(270)	
((293))	×	
((323))	×	
(360)	(361)	
398–425	398–425	
470	470	
×	511	
581	582	
×	((616))	
(686)	((686))	
(822)	×	Epoxy resin (Araldite)
((971))–988	971–988	Si–O and Al–O of Dvs
⟨1100⟩	⟨1100⟩	Si–O of the glass slide
(1612)	((1612))	Epoxy resin (Araldite)
⟨2845–2975⟩	⟨2845–2975⟩	C–H of the epoxy resin (Araldite)
(3069)	((3069))	C–H of the epoxy resin (Araldite)
n.d.	×	O–H around 3500 cm^{-1} = absent

n.d. = not determined; × = no significant signal.
⟨ ⟩ = wide; ___ = strong; ( ) = weak; (( )) = very weak.
Electronic spikes < 5 cm^{-1} wide are ignored.
Approx. laser power at the sample 5 mW (left) and 50 mW (right).
Counting time: 10 s. Accumulations: 5.

Hence there exists a risk of rejecting EMP analyses of Dvs as being poor analyses of sodic plagioclase. The situation is the same with Lis, whose chemical composition is similar to that of a more calcic plagioclase.

Furthermore, it is easy to miss crystals of Dvs or Lis in a matrix of hundreds small, low-to-medium birefringent, anhedral crystals in a thin section by conventionally supposing that they are all variously oriented plagioclase or quartz crystals. Taken together, these EMP and optical difficulties provide a credible and simple explanation why Dvs and/or Lis have not been reported from other retrogressed eclogite or {serpentine + jadeite-jade} local-

Table 4. The powder diffraction data (d in Å) for davidsmithite, compared with those measured for synthetic "Na-nepheline" and trinepheline (from the ICDD database). The strongest ten reflections are in bold. For davidsmithite, only peaks with $I_{rel} > 5$ are reported.

Davidsmithite This work			Na-nepheline[1] ICDD 00-035-0424			Trinepheline[2] ICDD 01-088-1231		
I_{rel}	d (calc)	$h\,k\,l$	I_{rel}	d (calc)	$h\,k\,l$	I_{rel}	d (calc)	$h\,k\,l$
9.7	8.645	0 1 0	7	8.640	1 0 0			
16.0	4.991	$\bar{1}$ 2 0	10	4.989	1 1 0			
27.4	**4.322**	**0 2 0**	**35**	**4.321**	**2 0 0**	**28.3**	**4.328**	**2 0 0**
65.7	**4.182**	**0 0 2**	12	4.280	1 1 1			
92.9	**3.840**	**0 2 1**	**80**	**4.165**	**0 0 2**	**56.1**	**4.133**	**0 0 6**
71.0	**3.267**	**$\bar{2}$ 3 0**	**100**	**3.834**	**2 0 1**	**87.8**	**3.834**	**2 0 3**
		$\bar{1}$ 3 0	70	3.266	2 1 0	42.5	3.272	1 2 0
20.5	3.042	$\bar{2}$ 3 1	**18**	**3.040**	**2 1 1**	18.7	3.163	2 1 2
100.0	**3.006**	**0 2 2**	**100**	**3.000**	**2 0 2**	16.6	3.042	2 1 3
41.3	**2.882**	**0 3 0**	**35**	**2.881**	**3 0 0**	**100.0**	**2.989**	**2 0 6**
23.2	**2.575**	**$\bar{2}$ 3 2**	**50**	**2.570**	**2 1 2**	**30.5**	**2.885**	**1 1 7**
		$\bar{1}$ 3 2				11.3	2.565	1 2 6
12.9	2.495	$\bar{2}$ 4 0	14	2.496	2 2 0	**20.3**	**2.498**	**2 2 0**
12.00	2.397	$\bar{3}$ 4 0	10	2.397	3 1 0	12.5	2.494	3 0 5
53.6	**2.343**	**0 2 3**	**35**	**2.336**	**2 0 3**	14.7	2.401	3 1 0
31.3	**2.305**	**$\bar{3}$ 4 1**	**25**	**2.304**	**3 1 1**	**31.9**	**2.324**	**2 0 9**
		$\bar{1}$ 4 1				**24.4**	**2.317**	**2 2 4**
10.9	2.121	$\bar{2}$ 3 3				**20.5**	**2.305**	**1 3 3**
		$\bar{1}$ 3 3						
17.4	2.091	0 0 4	16	2.083	0 0 4			
17.5	2.080	$\bar{3}$ 4 2	10	2.077	3 1 2			
		$\bar{1}$ 4 2						
5.1	1.983	$\bar{2}$ 5 0						
11.2	1.930	$\bar{3}$ 5 1						
5.3	1.883	$\bar{1}$ 5 0						
		0 2 4						
6.4	1.792	$\bar{2}$ 5 2						
5.2	1.708	0 4 3						
8.1	1.693	0 5 1						
6.5	1.634	$\bar{4}$ 6 0						
		$\bar{2}$ 6 0						
14.3	1.616	$\bar{3}$ 5 3						
		$\bar{2}$ 5 3						
7.0	1.598	0 5 2						
27.4	**1.561**	**$\bar{4}$ 5 3**	14	1.560	4 1 3	12.5	1.557	4 1 9
		$\bar{1}$ 5 3	14	1.555	2 0 5	14.6	1.544	3 3 6
		0 2 5	10	1.384	5 2 0			

[1] Space group $P6_3$, $a = 9.978$, $c = 8.330$ Å; Keller & McCarthy (1984).
[2] Space group $P6_1$, $a = 9.995$, $c = 24.797$ Å; calculated from Kahlenberg & Böhm (1998).

ities worldwide. One would have expected Dvs and/or Lis to have been recorded in some of the various published experimental petrology studies of Ca-rich, Si-poor and K-poor tectosilicate systems. Now the XRD pattern and Raman spectrum of Dvs are available for future studies. Notably, Leškevičiene & Nizevičiene (2010) could detect Lis in the dust from a cupola furnace in the same way.

5.2. Retrogressive reactions and possible petrogenetic environment

In any blueschist- or eclogite-facies mineral association that had been rich in jadeite and poor in quartz or coesite, the key retrogressive reaction amongst the tectosilicates in Ca-free zones would not be the classical reaction Jd + Qz = Ab but would be Jd = Ab + Trn. In the experimental literature, this reaction is almost always written with Nph instead of Trn, Jd = Ab + Nph, assuming purely sodic nepheline although Nph proper requires potassium.

With some Ca available in the system, this breakdown reaction of jadeite would form albitic plagioclase + Dvs. In more calcic zones with Ca available from the breakdown of the grossular component of garnet, or of the diopside component of omphacite, then Lis would form instead of, or as well as, Dvs. The associations of Dvs and Lis described here in sample G201b7, and also of Dvs and Trn found in another sample from Liset (D.C. Smith, pers. comm., 2017), both along with albitic plagioclase, fit the description above, exactly.
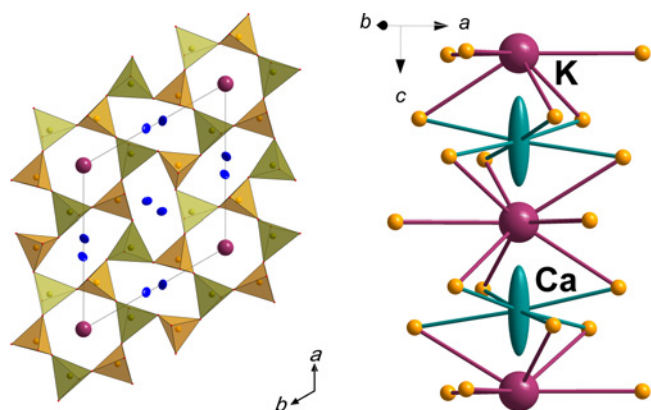
Fig. 4. The details of the crystal structure of davidsmithite relevant to the present discussion. The complete description has been reported in Rossi *et al.* (1989); (a) a layer of 6-membered rings of tetrahedra (projected on to $(0\,0\,0\,1)$), typical of the nepheline structure, half of which have hexagonal symmetry and may contain Na^+, K^+, or $(Ca^{2+}\square)$; (b) a pictorial representation of the electron density distributed along the 6-fold axis in these latter channels. Note the 6-fold coordination of the new Ca site, and the 9-fold coordination of the K site, the one typical of nepheline.

Table 5. Bond distance (Å) for davidsmithite before and after the correction for riding motion (Busing & Levy, 1964). The mean e.s.d. is 0.002 Å. Here the 9-fold coordinated site is labelled "K" since it has the same coordinates as the K site in classical nepheline. Ca is the new site for calcium. From Rossi *et al.* (1989).

	Uncorr.	Corr.		Uncorr.	Corr.
T1–O1	1.799	1.818	T2–O1	1.556	1.596
T1–O4	1.706	1.721	T2–O3	1.626	1.645
⟨T1–O⟩	1.729	1.745	⟨T2–O⟩	1.608	1.633
T3–O2	1.656	1.686	T4–O2	1.684	1.708
T3–O4	1.635	1.653	T4–O3	1.702	1.723
T3–O5	1.629	1.638	T4–O5	1.705	1.706
T3–O6	1.611	1.629	T4–O6	1.699	1.710
⟨T3–O⟩	1.633	1.651	⟨T4–O⟩	1.698	1.712
Na–O1	2.553	2.564	K–O2	3.056	3.044
Na–O2	2.504	2.508	K–O5	3.048	3,036
Na–O3	2.685	2.689	K–O6	2.983	2.973
Na–O3	2.753	2.753	⟨K–O⟩	3.029	3,018
Na–O4	2.871	2.874	Ca–O5	2.637	2.580
Na–O4	2.479	2.485	Ca–O6	2.797	2.749
Na–O5	2.506	2.508	⟨Ca–O⟩	2.715	2.664
Na–O6	2.579	2.581			
⟨Na–O⟩	2.616	1.818			

Two petrogenetic environments described for the creation of Lis in Smith *et al.* (1986) also apply here for Dvs. First, Na from jadeite and Al from kyanite and jadeite, coupled with a relatively low content of K and Mg in the whole of the Liset eclogite pod, undoubtedly contributed to the creation of the unusual (Na + Al)-rich phases Dvs, Lis and the nyböitic and taramitic amphiboles. Hence, the extreme Na–Al–K–Mg concentrations at Liset are the chemical criterion.

Second, the notable static retrogression that occurred at Liset (Smith, 1988) led to very little chemical mobility, many phases being armoured by coronas that prevented further reaction (*e.g.*, relict jadeite and quartz). In other words, the local lack of Si allowed the creation of feldspathoid rather than feldspar, and the local lack of K prevented the creation of classical nepheline.

Smith *et al.* (1986) and Smith (1988) estimated the *P–T* conditions for the formation of lisetite at very approximately $P = 10$ kbar at 700 °C, or at even higher pressure at the beginning of amphibolitisation in the Norwegian Coesite-Eclogite Province (Lappin & Smith, 1978; Smith, 1984). Such conditions would also be applicable to the formation of Dvs. Nothing is known about the stability of Dvs and Lis at lower *P* and lower *T* conditions. Apart from kinetic inhibitions, their survival at Liset suggests that they are stable as long as no more Si is available to allow the formation of Si-richer feldspar.

References

Boyer, H., Smith, D.C., Pinet, M. (1989): A comparison of the Raman spectra of some natural Ca–Al silicates. *in* "Georaman-89: contributions, special pub". Association Nationale de la Recherche Technique (ANRT), Paris, 3–4.

Bruker (2003): SAINT Software Reference Manual, ver. 6. Bruker AXS, Madison, WI.

Busing, W.R. & Levy, H.A. (1964): The effect of thermal motion on the estimation of bond lengths from diffraction measurements. *Acta Crystallogr.*, **17**, 142–146.

Chopin, C. (1984): Coesite and pure pyrope in high-grade blueschists of the Western Alps: a first record and some consequences. *Contrib. Mineral. Petrol.*, **86**, 107–118.

Deer, W.A, Howie, R.A., Zussman, J. (1992): The rock-forming minerals, 2nd edn. Longman Group, Harlow, Essex, UK, 696 p.

Ferraris, C., Parodi, G.C., Pont, S., Rondeau, B., Lorand, J.-P. (2014): Trinepheline and fabrièsite: two new mineral species from the jadeite deposit of Tawmaw (Myanmar). *Eur. J. Mineral.*, **26**, 257–265.

Hacker, B.R. (2007): Ascent of the ultrahigh-pressure Western Gneiss Region, Norway. *Geol. Soc. Am. Spec. Pap.*, **419**, 171–184.

Hansen, S. & Fälth, L. (1982): X-ray study of the nepheline hydrate I structure. *Zeolites*, **2**, 162–166.

Johan, Z., Martin, R.F., Ettler, V. (2017): Fluids are bound to be involved in the formation of ophiolitic chromite deposits. *Eur. J. Mineral.*, **29**, doi:10.1127/ejm/2017/0029-2648.

Kahlenberg, V. & Böhm, H. (1998): Crystal structure of hexagonal trinepheline – a new synthetic $NaAlSiO_4$ modification. *Am. Mineral.*, **83**, 631–637.

Kechid, S.A. (1984): Etude pétrologique et minéralogique des éclogites de Liset (Stadlandet, Norvège). Doctoral thesis, Univ. Paris VI et Muséum MNHN, Paris, France, 192 p.

Kechid, S.A. & Smith, D.C. (1985): The petrological evolution of the Liset eclogite pod, Norway. *in* "Second Internat. Eclogite Conf." *Terra Cogn.*, **5**, 422.

Keller, L. & McCarthy, G.J. (1984): JCPDS grant-in-aid report (International Center for Diffraction Data file no. 35-424).

Lappin, M.A. & Smith, D.C. (1978): Mantle-equilibrated orthopyroxene eclogite pods from the Basal Gneisses in the Selje District, Western Norway. *J. Petrol.*, **19**, 530–584.

Leškevičiene, V. & Nizevičiene, D. (2010): Anhydrite binder calcined from phosphogypsum. *Ceramics – Silikáty*, **54**, 152–159.

Oberti, R., Previde-Massara, E., Ungaretti, L., Kechid, S.-A., Smith, D.C. (1989): Nyböite–taramite–sadanagaite trend in amphibole from the Liset eclogite pod, Norway: crystal–chemical and petrogenetic implications. *in* "Third Internat. Eclogite Conf." *Terra Abstr.*, **1**, 17.

Oberti, R., Ungaretti, L., Tlili, A., Smith, D.C., Robert, J.-L. (1993): The crystal structure of preiswerkite. *Am. Mineral.*, **78**, 1290–1298.

Oberti, R., Boiocchi, M., Smith, D.C. (2003): Fluoronyböite from Jianchang (Su-Lu, China) and nyböite from Nybö (Nordfjord, Norway): description and comparison of two high-pressure amphibole end-members. *Mineral. Mag.*, **67**, 769–782.

Oberti, R., Boiocchi, M., Smith, D.C., Medenbach, O. (2007): Aluminotaramite, alumino-magnesiotaramite, and fluoro-alumino-magnesiotaramite: mineral data and crystal chemistry. *Am. Mineral.*, **92**, 1428–1435.

Rossi, G., Oberti, R., Smith, D.C. (1986): The crystal structure of lisetite. *Am. Mineral.*, **71**, 1378–1383.

—, —, — (1989): The crystal structure of a K-poor Ca-rich silicate with the nepheline framework and crystal–chemical relationships in the compositional space $(K,Na,Ca,D)_8(Al, Si)_{16}O_{32}$. *Eur. J. Mineral.*, **1**, 59–70.

Smith, D.C. (1976): The geology of the Vartdal Area, Sunnmöre, Norway, and the petrochemistry of the Sunnmöre Eclogite Suite. Ph.D. thesis, Aberdeen University, Scotland, UK, 1–750.

— (1984): Coesite in clinopyroxene in the Caledonides and its implications for geodynamics. *Nature*, **310**, 641–644.

— (1988): A review of the peculiar mineralogy of the "Norwegian coesite-eclogite province", with crystal–chemical, petrological, geochemical and geodynamical notes and an extensive bibliography. *in* "Eclogites and eclogite-facies rocks. Developments in petrology", D.C. Smith, ed. Elsevier, Amsterdam, vol. 12, 1–206, Chapter 1, 524 p.

Smith, D.C. & Lappin, M.A. (1982): Aluminium- and fluorine-rich sphene and clinoamphibole in the Liset eclogite pod, Norway. *in* "First Internat. Eclogite Conf." *Terra Cogn.*, **2**, 317–318.

Smith, D.C., Kechid, S.-A., Rossi, R. (1986): Occurrence and properties of lisetite, $CaNa_2Al_4Si_4O_{16}$, a new tectosilicate in the system Ca–Na–Al–Si–O. *Am. Mineral.*, **71**, 1372–1377.

Ungaretti, L., Smith, D.C., Rossi, G. (1981): Crystal-chemistry by X-ray structure refinement and electron microprobe analysis of a series of sodic–calcic to alkali-amphiboles from the Nybö eclogite pod, Norway. *Bull. Minéral.*, **104**, 400–412.

Ungaretti, L., Oberti, R., Smith, D.C. (1985): X-ray crystal structure refinements of ferro-alumino- and magnesio-alumino-taramites from the Liset eclogite pod, Norway. *Terra Cogn.*, **5**, 429–430.

Wain, A. (1997): New evidence for coesite in eclogite and gneisses: defining an ultrahigh-pressure province in the Western Gneiss region of Norway. *Geology*, **25**, 927–930.

Whitney, D.L. & Evans, B.W. (2010): Abbreviations for names of rock-forming minerals. *Am. Mineral.*, **95**, 185–187.